"IN-SITU" LASER RAMAN SCATTERING AND FAR INFRARED SPECTROSCOPY STUDIES OF CORROSION-PASSIVATION PHENOMENA IN METALS*

Carlos A. Melendres
Argonne National Laboratory
Argonne, IL 60439, USA

For publication in the Proceedings of the International Advanced Studies Institute on "Exploration of Subsurface Phenomena by Particle Scattering Techniques", Monterey, CA, October 19-23, 1998.

May 1999

*Work supported by the U.S. Department of Energy, Office of Environmental Management and Office of Energy Research under contract W-31-109-ENG-38.

DISCLAIMER

"IN-SITU" LASER RAMAN SCATTERING AND FAR INFRARED SPECTROSCOPY STUDIES OF CORROSION-PASSIVATION PHENOMENA IN METALS

Carlos A. Melendres
Argonne National Laboratory
Argonne, IL 60439, USA

ABSTRACT

Vibrational spectroscopic and electrochemical techniques are among the most useful tools for the elucidation of corrosion-passivation phenomena in metals. The former can provide information on the structure and composition of corrosion films "in situ" in aqueous solution environments, while thermodynamic and kinetic information may be obtained using electrochemical techniques. In this paper, we demonstrate the application of Laser Raman Scattering (LRS) and Synchrotron Far Infrared Reflectance Spectroscopy (SFIRS), coupled with electrochemical methods, for the determination of the structure and composition of surface films on nickel and copper in aqueous solution environment. The corrosion film on nickel has been found to consist of NiO and Ni $(OH)_2$ in the passive region of potential and NiOOH in the transpassive region. The film on copper consists of Cu_2O, CuO and $Cu(OH)_2$. We also show for the first time that SFIRS can be used to obtain information on the adsorption of ions on a metal surface with sub-monolayer sensitivity. Adsorption of Cl^-,Br^-, SO^{-2}, and PO_4^{-3} was found to occur at gold electrodes in perchloric acid solution. We also observed that when two different ions are present in solution, the more strongly adsorbed ion determined the corrosion behaviour of the metal.

INTRODUCTION

Vibrational spectroscopic techniques are increasingly used to study corrosion and passivation phenomena in metals. They provide molecular specific information than is otherwise obtainable from the interpretation of current-potential curves alone; hence, they

nicely complement thermodynamic and corrosion rate data obtained by electrochemical methods. These techniques have the advantage in their ability to examine materials and processes "in-situ" in the actual environment of interest. In contrast, conventional surface analytical techniques such as Electron Spectroscopy for Chemical Analysis (ESCA), Xray Photoelectron Spectroscopy (XPS), Auger Electron Spectroscopy (AES), Secondary Ion Mass Spectrometry (SIMS), etc, require the specimen to be in a high vacuum environment, which may cause some alteration of the sample.

Laser Raman Spectroscopy (Surface Enhanced Raman Spectroscopy or SERS, in particular) has been well established as a tool for the determination of the composition and structure of corrosion films on metals [1]. Infrared (IR) spectroscopy has also found a niche in the elucidation of interfacial electrochemical problems and processes because of its high surface sensitivity and the wide availability of commercial spectrometers [2]. A number of IR techniques have been developed for the study of electrochemical systems, but most of the work carried out has been in the mid IR region (600 to 4000 cm^{-1}). The rather low intensity of conventional laboratory sources (e.g. globar) and the strong absorption of IR radiation by water in the far IR region (below 600 cm^{-1}) account in part for the dearth of experimental work in this spectral region. The advent of synchrotron radiation sources, with about 1000 times higher intensity in the far IR region than globar [3], has opened up new opportunities for investigation in many fields. We present here some results that illustrate the utility of SFIRS for the study of the structure and composition of electrochemically formed surface films on copper, as well as the detection of adsorbed layers at a gold electrode surface. We will also describe recent applications of surface enhanced Raman spectroscopy (SERS) to determine the composition of surface films on nickel in aqueous solutions.

EXPERIMENTAL

Our setup for carrying out LRS has been described previously [1]. It consists essentially of a SPEX model 1403 double monochromator fitted with a photomultiplier tube detector. Data acquisition was by a SPEX Scamp Controller. A Coherent model Innova 300 Ar ion Laser was the source of the 514.5 nm line used for sample excitation.

Nickel electrodes for Raman spectroscopy studies generally consisted of 0.318 cm strips made from sheets of high purity (99.99%) nickel foil, 0.254-mm thick. These were polished with 600 grit emery paper, degreased with acetone, and rinsed repeatedly with water purified by passage through a reverse osmosis purification system. Surface enhanced Raman scattering was carried out using electrodeposited silver as described previously [4]. The electrochemical equipment consisted of a Princeton Applied Research (PAR) model 173 potentiostat/galvanostat driven by a PAR model 179 universal programmer.

For infrared experiments, we have used the far infrared beamline (U4IR) at the National Synchrotron Light Source (NSLS) of Brookhaven National Laboratory (Upton, NY).The facility is equipped with a Nicolet Impact 400 FTIR spectrometer hooked up to the UV ring which act as the source. For in-situ IR spectroelectrochemical experiments, an optical setup for extracting the IR beam, focusing it onto the electrode, and measuring the reflection-absorption spectra was devised and attached to the Nicolet spectrometer. This optical box was purged with dry nitrogen in order to minimize atmospheric interference during the spectral measurement.. The IR beam from the synchrotron was

polarized in the horizontal plane; advantage was taken of this fact by using electrodes oriented vertically. The copper electrodes for IR studies consisted of 10-mm diameter discs polished to optical finish using successive grades of alumina powder down to 0.05 micrometer. The disc electrode is embedded in a Teflon holder with a copper current collector lead. The electrochemical cell was made of Teflon and included counter and reference electrodes, as well as the electrolyte solution. It is of the conventional thin-layer type similar to that used by others. A silicon disc was used as the optical window.

For adsorption studies, the attentuated total internal reflectance (ATR) technique was employed. The electrode consisted of a 200 A Au film vacuum-deposited on a Si hemicylinder similar to that employed by Ataka, et al. [5]. Electrochemical measurements were carried out using conventional instrumentation. A saturated calomel electrode (SCE) was generally used as the reference; a mercury sulfate (MSE) was occasionally used where indicated, to avoid chloride contamination. The beam current in the 2.5 GeV synchrotron ring was normally in the range of about 800 to 300 mA during the measurements.

RESULTS AND DISCUSSION

Laser Raman Spectroscopy

A cyclic voltammogram of nickel in 0.1 M NaOH solution is shown in Fig.1. Two anodic waves I and II are evident in the region of anodic dissolution of nickel to Ni^{2+}. The waves IIIa and IIIc correspond, respectively, to the formation of a higher valency nickel species and its subsequent reduction. We first consider the surface species in the active dissolution and passive potential regions, which give rise to a very thin passive film that is difficult to characterize spectroscopically. The interpretation of the two anodic waves in nickel dissolution has varied widely. MacDougall and Cohen [6], for example, attribute wave II to the presence of impurities in solution. We have always observed waves I and II in voltammograms of nickel in different solution environments even without sulfate present; others have also [7,8]. We will show that they are not due to artifacts but correspond to the formation of $Ni(OH)_2$ and NiO respectively. This assignment follows from a correlation of the surface-enhanced Raman spectra observed and the cyclic voltammogram that is discussed below.

The passive film on nickel is less than 20 A thick, as had been measured by various workers using ellipsometry. Our attempts to obtain normal Raman spectra have not been successful, and it was necessary to employ the surface-enhanced Raman effect using a silver overlayer on the nickel surface.The particle size of the electrodeposited silver appears to be in the order of about 500-1000 A, and scanning electron photomicrographs show that the surface is not completely covered by the silver [4]. No attempt was made here to optimize the coverage to obtain maximum surface enhancement; we found little difference in SERS intensity between 10 and 30 mC/cm^2 of silver loading. Figure 2 shows the effect of the silver overlayer on the voltammogram of nickel in 0.1 M NaOH. The anodic waves I and II remain virtually unchanged, but a cathodic wave becomes prominent at about -0.4 V. This wave is due to the reduction of

dissolved oxygen, which is catalyzed by silver. The waves at about 0.25 V correspond to the oxidation and reduction of the electrodeposited silver.

Figures 3(a) - 3(e) show in-situ surface-enhanced Raman spectra of the nickel electrode in 0.1M NaOH solution as a function of applied potential. Following the electrodeposition of silver and pre-cleaning of the electrode at -1.3 V for 15 min, the "in-situ" spectrum of the surface was obtained while holding the electrode at -1.0 V for 1 h. This is shown in Fig. 3(a). The absence of a discernible Raman band indicates that the surface is relatively free of an oxide or hydroxide film initially at this potential. On increasing the potential to -0. 8 V (in the pre-passive region of Fig. 3), a band at about 450 cm^{-1} starts to appear, indicating the formation of a surface film. This band is assigned to the Ni-OH vibration of $Ni(OH)_2$ in accordance with the work of Desilvestro et al [9]. The latter have studied extensively the surface-enhanced Raman spectra of $Ni(OH)_2$ prepared by cathodic deposition on a roughened gold electrode. Further confirmation of the correctness of this assignment is the observation of the OH stretching vibration of $Ni(OH)_2$ at about 3630 cm^{-1}, as shown in Fig. 4. On scanning the potential further and holding at -0.4 V (past wave II in the voltammogram of Fig. 1), we obtained the in-situ spectra shown in Fig. 3(c). A new band is evident at about 512 cm^{-1}, together with the old band at 456 cm^{-1}. We assign this new band to NiO by comparison with the spectrum of standard reagent grade NiO. Increasing the potential to 0 V resulted only in an increase in intensity of the two bands [Fig. 3(d)], presumably owing to an increase in the thickness of the corresponding surface films with potential. A corresponding increase in intensity of the OH vibration is also observed [Figs. 4(b) and 4(c)]. On reversing the voltammetric scan and holding the potential at -0.9 V, a considerable reduction in the intensity of the bands at 450 and 510 cm^{-1} is observed [Fig. 3(e)]. The bands, however, do not completely disappear even after 2 h, suggesting slow kinetics or some irreversibility in the reduction of the film.

The principal results presented thus far are: (1) the observation of the presence of both $Ni(OH)_2$ and NiO in the surface film(s) on nickel in the passive region of potential for the alkaline solutions studied and (2) the correlation between the formation of $Ni(OH)_2$ with the first anodic wave (I) and that of NiO with the second (II) in the current-potential curve for nickel. There has been no general consensus on the composition of the passive film on nickel despite over 50 years of research investigations. Some [10] claim that the film is $Ni(OH)_2$ while others [11,12] believe that it is NiO. X-ray photoelectron spectroscopy (XPS) studies [13] "ex situ" have led to the conclusion that both species are present on the electrode surface. Our results show unequivocally that both NiO and $Ni(OH)_2$ are present in the surface film in the passive potential region. We also show that $Ni(OH)_2$ is first formed which supports the contention of Bockris et al.[14] that it constitutes what they refer to as the "pre-passive" film; NiO is formed at more positive potentials. These results are consistent with the standard potentials calculated for the reaction

$$NiO + 2H^+ + 2\,e^- \rightarrow Ni + H_2O \qquad E' = -0.6\ V \text{ at pH } 12 \qquad (1)$$

given by Pourbaix [15] and that given by Hoare [16] for the formation of $Ni(OH)_2$, i.e.,

$$Ni(OH)_2 + 2\,e^- \rightarrow Ni + 2OH^- \qquad E' = -0.72\ V. \qquad (2)$$

While the Raman technique does not allow us to distinguish between a model of the passive film consisting of a homogeneous mixture of NiO or $Ni(OH)_2$ or a duplex film, it is nevertheless useful to theorize on the structure of the passive film based on our spectroscopic and electrochemical results, as well as those of others. Our results are consistent with a bilayer model in which the $Ni(OH)_2$ layer is first formed by a dissolution-precipitation type mechanism. We then envisage an inner film composed of NiO to be formed by a solid state mechanism on the metal surface at a more positive potential. Both layers grow in thickness at higher potentials, as indicated by an increase in the Raman intensity of both 450 and 510 cm^{-1} bands with potential. Such a duplex-type model has been used earlier by Hoppe and Strehblow [13] in interpreting the results of their XPS measurements. They were able to calculate the thickness of the NiO and $Ni(OH)_2$ layers at different potentials, although it should be noted that these are measurements under high vacuum conditions. A structural model in which the film is composed of a mixture of $Ni(OH)_2$ and NiO is also possible and cannot be differentiated by the Raman technique from the duplex film model. It appears, however, that the latter would be most consistent with the results of others as well as our own. Finally, it is also important to point out here that neither of the two anodic waves observed during the dissolution of nickel is due to impurities or artifacts. These waves correspond to the formation of $Ni(OH)_2$ and NiO, respectively. NiO is formed independently of $Ni(OH)_2$ rather than as a result of the conversion (e.g., by dehydration) of the pre-passive film, as Bockris et al.[14] and Paik and Szklarska-Smialowska [10] have hypothesized. This is the first time that this correlation has been made and shows the power of "in-situ" spectroscopic techniques in quantifying mechanistic details of electrochemical reactions not otherwise obtainable from current-potential measurements alone. Moreover, the present work also attests to the utility of the surface enhanced Raman effect, albeit still limited to the use of a few metals such as silver, copper, and gold. The possibility of enhancing weak Raman signals via the electrodeposition of an overlayer of these SERS metals greatly extends the usefulness of the technique in electrochemical applications.

The composition of the corrosion film on nickel in the transpassive region (corresponding to the anodic wave at about + 0.5 V in Fig. 2) is also of interest and has great significance in the operation of nickel-based batteries. Melendres and Xu [17] were the first to obtain the Raman spectrum of the transpassive film on nickel. No surface enhancement via metal deposition was needed, the film being considerably thicker than the passive film and probably exhibiting a resonance Raman effect. The spectrum consisted of a doublet with band frequencies of 478 and 554 cm^{-1} (Fig. 5). We had originally assigned this band to a hydrated form of nickel oxide i.e., $Ni_2O_{3.4}$ $2H_20$. We now believe that a better formulation would be NiOOH on the basis of our more recent X-ray Absorption Spectroscopy investigations [18] .

Synchrotron Far Infrared Reflection Spectroscopy Studies

The spectroelectrochemical behavior of copper was studied in deaerated 0.1 M NaOH solution. Figure 5 shows a voltammogram of Cu in 0.1 M NaOH under the conditions of the spectroscopy experiment. It is similar to that published by Mayer and

Mueller [19]. They attributed the first anodic wave A1 to the formation of Cu_2O on the basis of their Raman results. Our infrared measurements at -0.3 V vs. SCE did not yield a spectrum. It must be remarked though, that the amount of charge under A1 is about 0.5 mC/cm^2. This would be equivalent to about 1 monolayer of material and appears to be below the detection capability of the specular reflection technique at present. At - 0.05 V, we obtained the "in-situ" spectrum shown in Fig. 6a. The bands at 630, 790 and 1110 cm^{-1} are assigned to Cu_2O, which is in reasonable agreement with the results of others [5,6]. At + 0.30 V, the far IR spectrum of Cu "in-situ" shows several bands as can be seen in Fig.6b. (Note that a reflectance greater than 100 comes about because of the decay of the synchrotron beam current; only the relative change in reflectance is important in judging the intensity of the signal.) At potentials above -0.2 V, we expect further oxidation of Cu to proceed forming such products as CuO and $Cu(OH)_2$. Formation of these species has been indicated by the Raman measurements of both Hamilton [22] and Mayer [19], but their technique could not detect CuO. Far IR spectra of bulk CuO, however, have been obtained by a number of workers [21,22]. Poling [20] observed a broad band at about 510 cm^{-1}. Narang et al [23] showed a multiplet of six bands at 147, 163, 324, 444, 515, and 586 cm^{-1}. We have measured the far IR spectrum of bulk $Cu(OH)_2$ as a powder in Nujol mull by using a conventional IR spectrometer in our laboratory . Using it as a reference [24], it is apparent that the 240, 422, and 486 cm^{-1} bands in our "in-situ" spectrum are due to the presence of $Cu(OH)_2$. The passive film at 0.3 V thus consists of a mixture of CuO and $Cu(OH)_2$.

In the investigation of corrosion and passivation phenomena in metals, techniques for detecting adsorption at electrodes "in situ" would be of great utility. It was of interest for us to determine the limit of detection sensivity of the SFIRS technique by examining adsorption processes at electrodes. Gold was the electrode of choice because of its inertness and the availability of information on its use for attenuated total internal reflection work. We examined the adsorption of chloride, bromide, nitrate, sulfate and phosphate from perchloric acid solutions.

Fig. 7 shows cyclic voltammograms of the 200 A Au film-on-Si electrode in the double layer region in 0.5 M perchloric acid solution (broken line) as well as in a solution containing 0.05 M KCl (solid line). The small adsorption/desorption waves at about 0.5 V vs SCE in the pure solution most probably correspond to perchlorate ion as had been proposed by Ataka et.al. [5]. In the presence of 0.005 to 0.05 M KCl in solution, an additional set of waves appears at about 0.3 V, which we believe corresponds to the adsorption and desorption of Cl^-. Figure 8a shows the far IR spectrum obtained at a potential of 0.45 V (referred to the condition of the electrode at –0.1 V). The band at about 263 cm^{-1} is assigned to the vibrational stretching mode of Au-Cl on the electrode surface. This assignment agrees well with that made by Gao and Weaver [25] who observed the adsorption of halide ions on Au using the technique of surface enhanced Raman spectroscopy (SERS). It is worthwhile to note the quality of the signal obtained by the SFIRS technique. The signal strength is about 0.3% with a background noise level of about 0.03%. This is only with co-adding 9 spectra. The total coulombic charge measured in taking the potential from –0.1 to 0.45 V was 0.083 mC/cm^2. This amount of charge associated with the adsorption process corresponds to the involvement of no more than a monolayer amount of material. Despite lack of knowledge of the surface structure

of our gold electrode, we can get an estimate of the degree of surface coverage by the adsorbate. We assume the number of gold atoms on the surface to be 1.39×10^{15} per cm^2, which is equal to that on the Au (111) plane with the highest packing density of surface atoms. The charge required to form a monolayer [26] of species occupying one site and requiring one electron per site is 0.222 mC/cm^2 .The charge of 0.083 mC/cm^2 attendant to the adsorption of Cl^- would then correspond to a surface coverage of 0.37. Even allowing for surface disorder, a coverage of about 0.5 would not be unreasonable and leaves little doubt that the SFIRS technique is sufficiently sensitive to detect adsorbates on electrodes "in situ" at monolayer and sub-monolayer levels

We have likewise obtained the far IR spectrum of Br^- adsorbed on Au in 0.5 M perchloric acid with 0.05 M NaBr (Fig. 8b). The center frequency of the band was measured at 187 cm^{-1} which is in reasonable agreement with the shift from the Au-Cl frequency that would be expected on the basis of the ratio of the reduced masses of Br and Cl. It is also in good agreement with the value of 185 cm^{-1} for surface-adsorbed Br^- obtained by Gao and Weaver [25] from SERS measurements on Au. We have also measured the SFIRS of nitrate, sulfate, and phosphate in 0.05 M solutions of KNO_3, Na_2SO_4, and Na_3PO_4 in 0.5 M $HClO_4$. The results are shown in Fig. 9. There appears to be little or no adsorption of nitrate, but bands due to adsorbed sulfate and phosphate are clearly evident. On the basis of mid IR work done by Weber and Nart [27,28], it is likely that the latter two anions are bonded to the gold surface through the oxygen; thus the far infrared frequencies observed differ only slightly. We studied the co-adsorption of bromide and phosphate on gold from a solution of 0.5 M perchloric acid containing 0.05 M each of NaBr and Na_3PO_4. We found that the current-potential behavior is determined by the more strongly adsorbed anion (bromide) as illustrated in Fig. 10. The SFIRS showed bromide to be adsorbed on the gold surface, apparently displacing the phosphate ion. The aggressive nature of halides in inducing corrosion correlates well with its strong adsorption characteristic.

ACKNOWLEDGMENT

This work was supported by the Division of Environmental Management Science and Division of Materials Science, U.S. Department of Energy, under contract W-31-109-ENG-38. The synchrotron measurements were carried out at the National Synchrotron Light Source at Brookhaven National Laboratory. Additional support to F. Hahn, J. M. Leger and B. Beden by a NATO Collaborative Research Grant No. 920512, as well as a CNRS-NSF exchange program, is also gratefully acknowledged. G.A. Bowmaker was supported by a grant from the University of Auckland Research Grants Committee. We thank G.P. Williams, D. VanCampen, and L. Miller for their assistance in the operation of the U4IR beamline facility and for many helpful discussions.

REFERENCES

1. C. A. Melendres, in Electrochemical and Optical Techniques for the Study and Monitoring of Metallic Corrosion, M.G.S.Ferreira and C.A. Melendres (eds), NATO-ASI Series E-vol.**203**, Kluwer Academic Publishers, Dordrecht, the Netherlands, (1992), p. 355.
2. B. Beden, in Spectroscopic and Diffraction Techniques in Interfacial Electrochemistry C. Gutierrez and C.A. Melendres (editors), NATO ASI Series C, vol. **320**, Kluwer Academic Publishers, Dordrecht, the Netherlands, (1990) p. 181.
3. C. J. Hirschmugl and G. P. Williams, in Synchrotron Techniques in Interfacial Electrochemistry, C.A. Melendres and A. Tadjeddine (editors),NATO ASI Series C, vol. **432**, Kluwer PublishersDordrecht, The Netherlands (1994).
4. C.A.Melendres and M. Pankuch, J. Electroanal. Chem. **333**,103 (1992)
5. K. Ataka, T. Yotsuyanagi, M. Osawa, J. Phys. Chem. **100**, 10664 (1996).
6. B. MacDougall and m. Cohen, J. Electrochem. Soc. **123**, 191 (1976).
7. W. Visscher and E. Berendrecht, Surf. Sci. **135**, 436 (1983).
8. J. H. Gerretsen and J. H. DeWit, J. Appl. Electrochem. **21**, 276 (1991).
9. J. Desilvestro, D.A. Corrigan and M. J. Weaver, J. Electrochem. Soc. **135**, 885 (1988).
10. W. Paik and S. Smialowska, Surf. Sci. **96**, 401 (1980).
11. R. Cortes, M. Froment, A. Hugot-LeGoff, and S. Joiret, Corros. Sci. **31**, 121 (1990).
12. D.D. MacDonald, R. Y. Liang, and B. G. Pound, J. Electrochem. Soc. **134**, 2981 (1987).
13. H. W. Hoppe and H. H. Strehblow, Surf. and Interface Anal. **14**, 121 (1989).
14. J. O'M Bockris, A. K. N. Reddy, and B. Rao, J. Electrochem. Soc. **113**, 1133 (1966).
15. M. Pourbaix, Atlas of Electrochemical Equilibria in Aqueous Solutions, Pergamon, Oxford (1966).
16. J.P. Hoare, The Electrochemistry of Oxygen, Interscience, NY (1968), p.276
17. C. A. Melendres and S. Xu, J. Electrochem. Soc. **131**, 2239 (1984).
18. A.N. Mansour, C.A. Melendres, M. Pankuch, and R.A. Brizzolara, J. Electrochem. Soc. **141**, L69 (1994).
19. S.T. Mayer and R.H. Mueller, J. Electrochem. Soc. **139**, 426 (1992).
20. G.W. Poling, J. Electrochem. Soc. **116**, 958 (1969).
21. D. Persson and C. Leygraf, J. Electrochem. Soc. **140**, 1256 (1993)
22. J.C. Hamilton, J.C. Farmer, and R.J. Anderson, J. Electrochem. Soc. **133**, 739 (1986).
23. S.H. Narang, V.B. Kartha, and N.D. Patel, Physica C **204**, 8 (1992).
24. C.A.Melendres, G.A. Bowmaker, J. M. Leger, B. Beden, J. Electroanal. Chem. **449**, 215 (1998).
25. P. Gao and M. Weaver, J.Phys. Chem. **90**, 4057 (1986).
26. H. Angerstein-Kozlowska, B.E. Conway, A. Hamelin, L. Stoicoviciu, J. Electroanal . Chem. **228**, 429 (1987).
27. M. Weber and F.C. Nart, Langmuir,**12**, 1895 (1996).
28. M. Weber and F.C. Nart, Electrochim. Acta, **41**, 653 (1996).

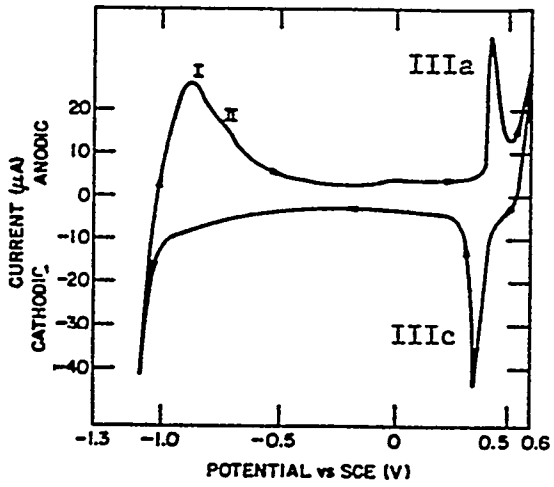

Figure 1. Cyclic voltammogram of Nickel in 0.1 M NaOH solution (scan rate= 5 mV/sec).

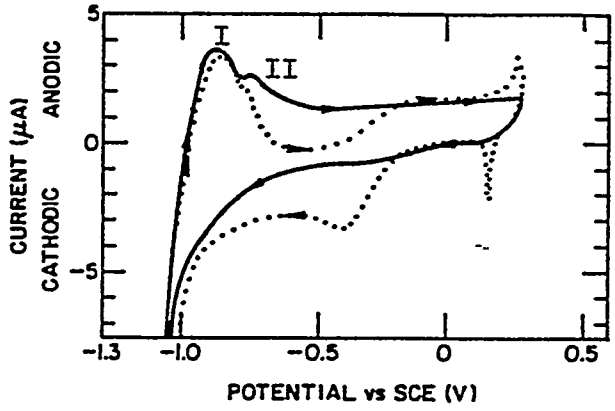

Figure 2. Effect of electrodeposited Silver on the cyclic voltammogram of Nickel in 0.1 M NaOH solution (scan rate, 5 mV/sec); ___, without a Silver overlayer ; .....,with a Silver overlayer.

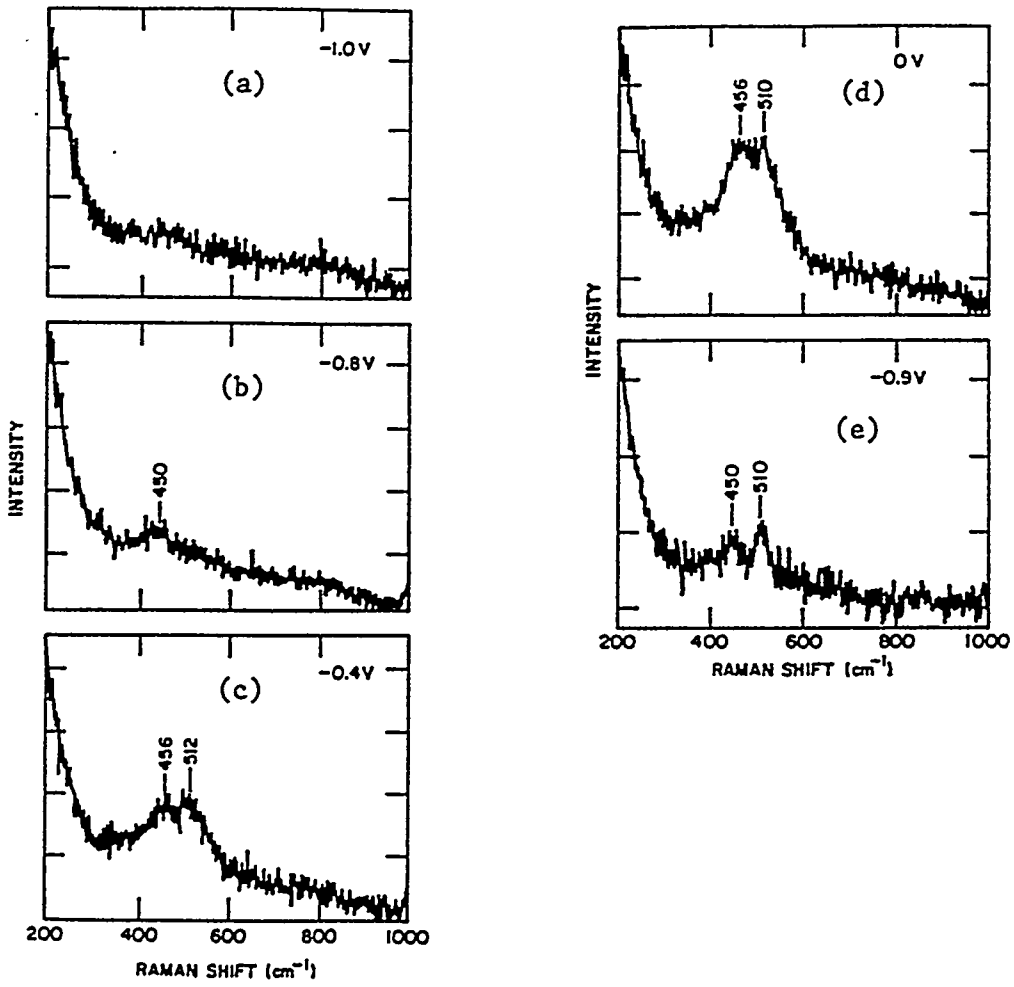

Figure 3 Laser Raman spectra of Nickel in 0.1 M NaOH solution at various potentials (Ar^+ laser; 514.5 nm line; P = 100 mW).

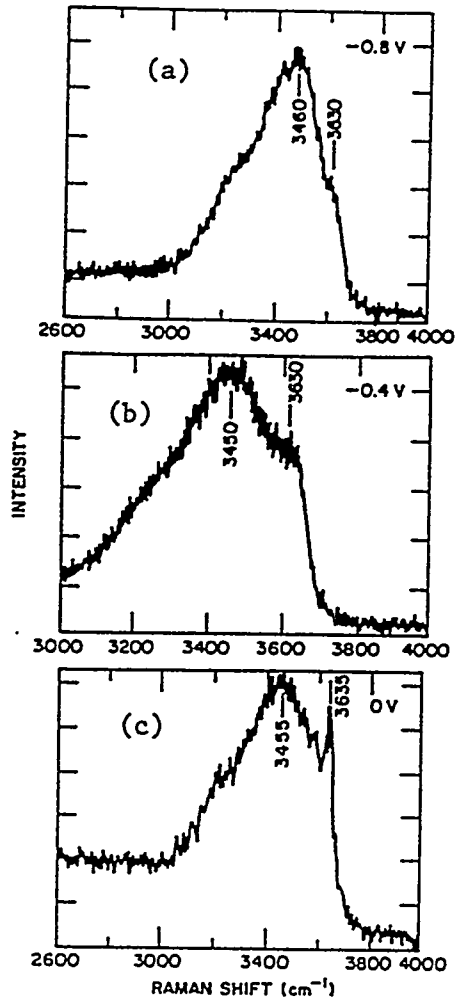

Figure 4. Laser Raman spectra of Nickel in the OH stretching region.

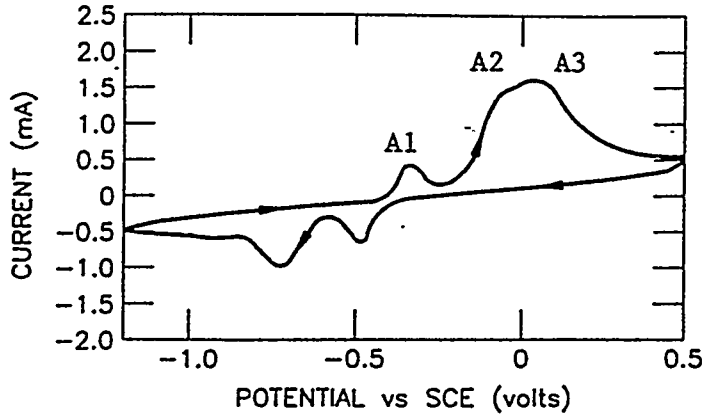

Figure 5. Cyclic voltammogram of Copper in de-aerated 0.1 M NaOH solution (scan rate = 20 mV/s)

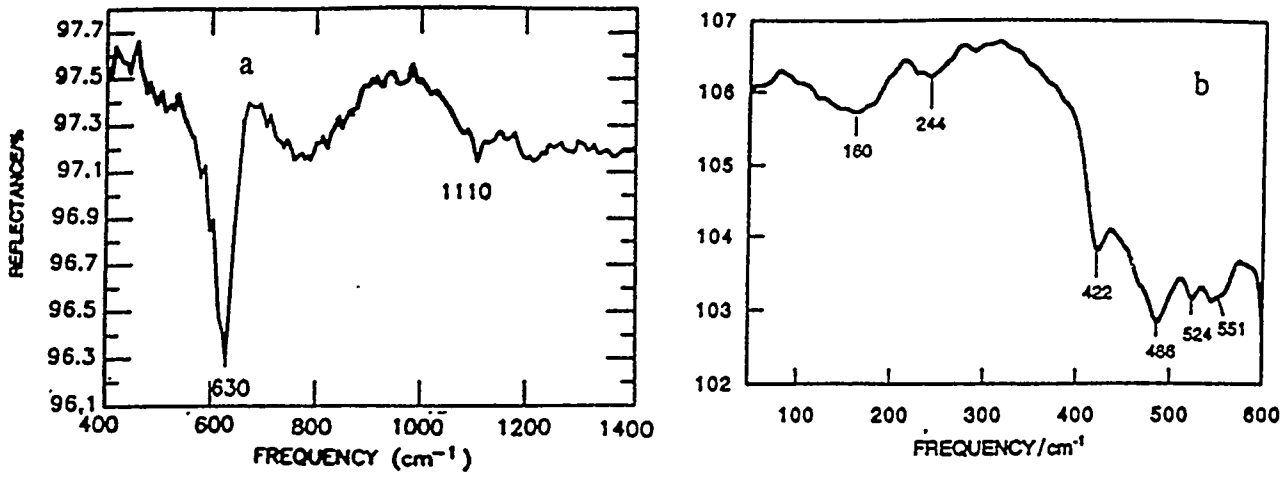

Figure 6. "In-situ" IR spectrum of Copper in 0.1 M NaOH (a) at –0.05 V vs. SCE (referenced to spectrum at –0.9 V), (b) at 0.3 V (referenced to –1.0V)

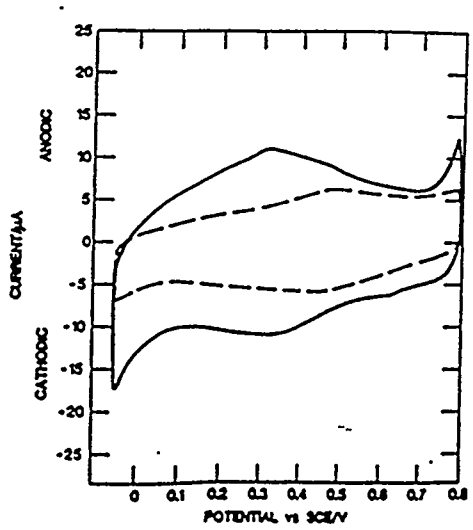

Figure 7. Cyclic voltammograms of a Gold thin film electrode in 0.5 M perchloric acid (broken line) and in 0.05 M KCl + 0.5 M perchloric acid (solid line); scan rate = 50 mV/s .

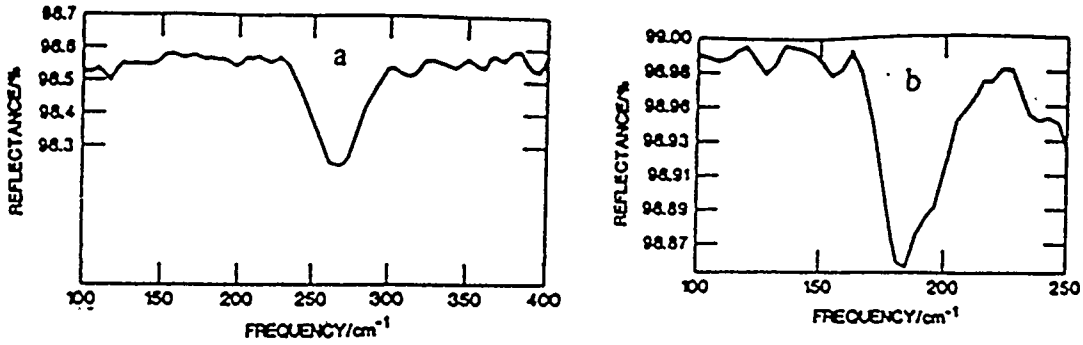

Figure 8. "In-situ" Synchrotron far IR spectra of a Gold electrode (a) in 0.5 M perchloric acid + 0.05 M KCl with applied potential, E=0.45 V vs SCE (reference at 0.1V), (b) in 0.5 M perchloric acid + 0.05 M NaBr, E=0.5 V (reference at – 0.3 V).

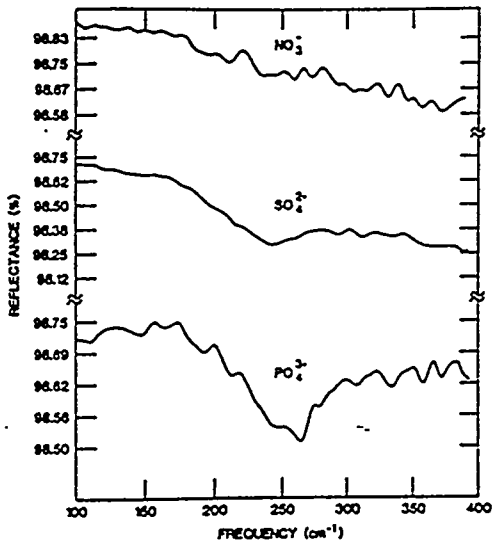

Figure 9. "In situ" synchrotron far IR spectrum of a Gold electrode in 0.5 M perchloric acid + 0.05 M of KNO_3, Na_2SO_4, and Na_3PO_4 , respectively; E= 0.5 V (reference at -0.5 V).

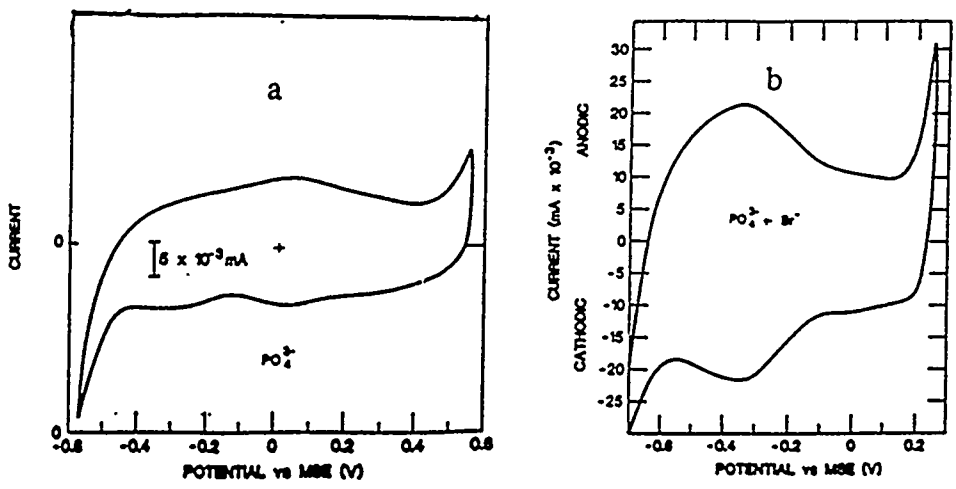

Figure 10. Cyclic voltammogram of Gold (a) in 0.5 M perchloric acid + 0.05 M Na_3PO_4 b) in 0.5 M perchloric acid + 0.05 M NaBr + 0.05 M Na_3PO_4 ; scan = 50 mV/sec